A NEW STEADY-STATE ANALYSIS METHOD FOR NONLINEAR CIRCUITS DRIVEN BY MULTI-TONE SIGNALS

Lucia DUMITRIU, Mihai IORDACHE

„Politehnica" University of Bucharest, Electrical Engineering Department,
dlucia@elth.pub.ro, iordache@elth.pub.ro

***Abstract* – The paper presents a new version of the modified nodal method for analysis of the circuits with widely separated time scales. The key idea is to use multiple time variables, which enable signals with widely separated rates of variation to be represented efficiently. The differential algebraic equations (DAE) describing the RF-IC circuits are transformed in multi-time partial differential equations (MPDE). In order to solve MPDE we use the associated resistive discrete equivalent circuits (companion circuits) for the dynamic circuit elements. The algorithm to formulate and to solve the dynamic modified nodal equations was implemented in a computing program, which constitutes a useful tool for steady-state analysis of a very large class of nonlinear analog circuits.**

Keywords: *nonlinear analog circuit, multi-tone signal, multi-time partial differential equation.*

1. INTRODUCTION

A typical RF-IC application has carrier frequencies in the GHz-range with modulating signals in the kHz-range. Such signals are called *multirate signals*, and they contain "components" that vary at two or more widely separated rates. These systems are typically difficult to analyze using traditional numerical integration algorithms, such as those in programs like SPICE [1]. The difficulty comes from the widely disparate rates: following fast-varying signal components long enough to obtain information about the slowly-varying ones is computationally expensive, and can also be inaccurate. So finding the steady-state by the brute-force method is, in this case, time-consuming [1, 2].

Many multirate signals, especially from circuits, can be represented efficiently as functions of two or more time variables, i.e., as *multivariate functions*. If a circuit is described with differential-algebraic equations (DAE), using multivariate functions for the unknowns naturally leads to a partial differential equation (PDE) form, called *Multirate Partial Differential Equations* (*MPDE*). If we apply time-domain numerical methods to solve the MPDE directly for the multivariate forms of the unknowns, we are able to analyze the combination of strong nonlinearities and multirate signals.

The Modified Nodal Equations (MNE) in dynamic behavior and the output equation for lumped nonlinear analog circuits have the following form [11-13]:

$$\begin{cases} \boldsymbol{M}\left(\boldsymbol{x}(t)\right)\cdot\dot{\boldsymbol{x}}(t)+\boldsymbol{G}\boldsymbol{x}(t)+\boldsymbol{F}\left(\boldsymbol{x}(t)\right)=\boldsymbol{B}\boldsymbol{y}(t) \\ \boldsymbol{u}(t)=\boldsymbol{L}^{\mathrm{t}}\boldsymbol{x}(t) \end{cases}, \quad (1)$$

where: $\boldsymbol{x}(t)=\left[\boldsymbol{v}_{n-1}^{\mathrm{t}},\boldsymbol{i}_{m}^{\mathrm{t}}\right]^{\mathrm{t}}$ - is the independent variable vector, with $\boldsymbol{x}_0$ initial condition; $\boldsymbol{M}$, $\boldsymbol{G}$ are square matrices $(n-1+m)\times(n-1+m)$; $\boldsymbol{y}=\left[\boldsymbol{j}^{\mathrm{t}},\boldsymbol{e}^{\mathrm{t}}\right]^{\mathrm{t}}$ - is the input vector; *F*- represents the resistive terms; *B* and *L* are selector matrices, with entries (–1, 0 or 1), and the superscript "t" denotes the transpose.

If for the nonlinear inductors (nonlinear capacitors) the magnetic fluxes (electrical charges) are considered as the independent variables, then the matrix *M* is independent of *x*. The circuits exhibiting multirate behavior can be efficiently represented using multiple time variables. If there are *p* multivariate forms of change, *p* time-scales are used. We denote the multivariate forms of *x*(*t*) and *b*(*t*) by $\hat{\boldsymbol{x}}\left(t_1,\ldots,t_p\right)$ and $\hat{\boldsymbol{b}}\left(t_1,\ldots,t_p\right)$.

The MPDE corresponding to (1) is:

$$\begin{cases} \boldsymbol{M}\left(\hat{\boldsymbol{x}}\right)\left[\dfrac{\partial\hat{\boldsymbol{x}}}{\partial t_1}+\ldots+\dfrac{\partial\hat{\boldsymbol{x}}}{\partial t_p}\right]+\boldsymbol{G}\hat{\boldsymbol{x}}+\boldsymbol{F}\left(\hat{\boldsymbol{x}}\right)=\boldsymbol{B}\hat{\boldsymbol{b}}\left(t_1,\ldots,t_p\right) \\ \hat{\boldsymbol{u}}\left(t_1,\ldots,t_p\right)=\boldsymbol{L}^{\mathrm{t}}\hat{\boldsymbol{x}}\left(t_1,\ldots,t_p\right) \end{cases} \quad (2)$$

A relation between MPDE and MNE is proved to be in [1]. According to the theorem 1 from [1] the solutions of MNE are available on the "diagonal" lines a long the MPDE multivariate solutions.

The modified nodal equations (MNEs) are very easy to formulate and to implement into a program [4,7,8,9]. Replacing each capacitor and inductor (magnetic coupled or not) by a discrete resistive circuit model associated with an implicit numerical integration algorithm, efficiency in numerical computing of the associated MPDE is obtained. The characteristics of the nonlinear circuit elements are approximated by piecewise-linear continuous curves [5-10].

By using the backward differential formula of high order, the efficiency is achieved without compromising accuracy.

2. NUMERICAL METHOD TO SOLVE MPDE

We consider the two-rate case. The MPDE (2) becomes:

$$\begin{cases} \boldsymbol{M}(\hat{\boldsymbol{x}})\left[\dfrac{\partial \hat{\boldsymbol{x}}}{\partial t_1}+\dfrac{\partial \hat{\boldsymbol{x}}}{\partial t_2}\right]+\boldsymbol{G}\hat{\boldsymbol{x}}+\boldsymbol{F}(\hat{\boldsymbol{x}})=\boldsymbol{B}\hat{\boldsymbol{b}}(t_1,t_2) \\ \hat{\boldsymbol{u}}(t_1,t_2)=\boldsymbol{L}^{\mathrm{t}}\hat{\boldsymbol{x}}(t_1,t_2) \end{cases} \quad (3)$$

with the periodic boundary conditions (BCs) $\hat{\boldsymbol{x}}(t_1+T_1,t_2+T_2)=\hat{\boldsymbol{x}}(t_1,t_2)$. We take a uniform grid $\{\bar{t}(i,j)\}$ of size (n_1+1)x(p_2+1) on the rectangle [0, m_1T_1]x[0,T_2] (Fig.1), where $\bar{t}(i,j)=(t_{1\_i},t_{2\_j})$, with $t_{1-i}=(i-1)h_1$, t_{2_j} = (i-2)T_2+(j-1)h_2, $i=\overline{1,n_1+1}$, $j=\overline{1,p_2+1}$; $h_1=m_1T_1/n_1$ = T_1/p_1, and $h_2=T_2/p_2$. Consider that the slow components of $\boldsymbol{b}(t)$ and $\boldsymbol{x}(t)$ depend on t_1 and the fast components of $\boldsymbol{b}(t)$ and $\boldsymbol{x}(t)$ depend on t_2.

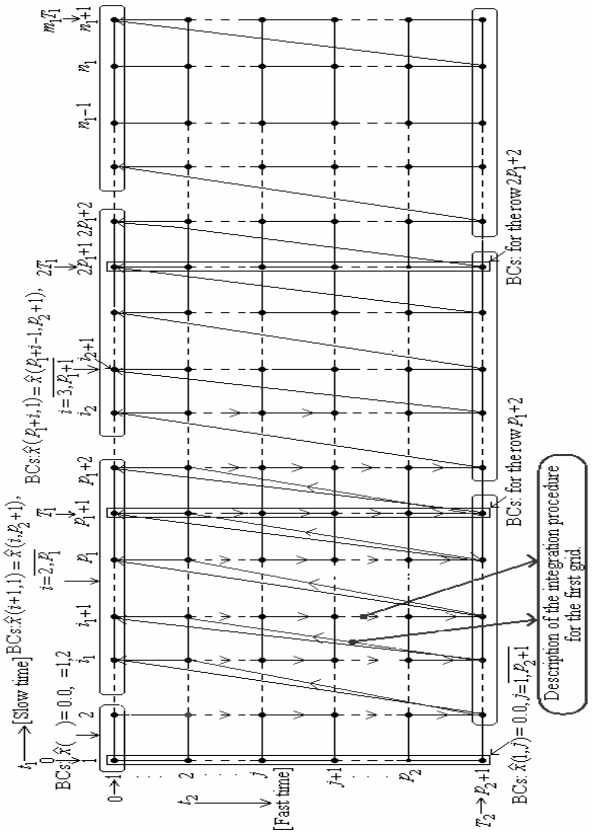

Fig. 1: A uniform grid $\{\bar{t}(i,j)\}$ of size $(n_1+1)\times(p_2+1)$.

According to the *backward differential formula* (BDF), which approximates into the range of any prescribed accuracy, the present value $\dot{x}(t_q)=\dot{x}_q$ at $t=t_q$ in terms of $x_q=x(t_q)$ and p values $x_{q-1},x_{q-2},...,x_{q-p}$, $\dot{x}_q$ has the following expression:

$$\dot{x}=\frac{1}{h}\sum_{k=0}^{p}a_k x_{q-k}\ , \quad (4)$$

where $a_0,a_1,...,a_p$ are constants, and $h=t_q-t_{q-1}$ is the present time step size.

For the first periods T_1 and T_2 (corresponding to the grid of size (p_1+1)x(p_2+1)), we assume that the BCs are $\hat{\boldsymbol{x}}(1,j)=0.0$, $j=\overline{1,p_2+1}$ and $\hat{\boldsymbol{x}}(i,1)=0.0$, i=1,2; and $\hat{\boldsymbol{x}}(i+1,1)=\hat{\boldsymbol{x}}(i,p_2+1)$, $i=\overline{2,p_1}$; on the row t_1 = 0, and on the column t_2 = 0 respectively. We start the integration process on the row 2 from the point $\bar{t}(2,2)=(t_{1\_2},t_{2\_2})$, with $t_{1\_2}=h_1$, $t_{2\_2}=h_2$ (in respect of the fast time t_2) from the column 2 to the column p2+1 and so on till we arrive in the point $\bar{t}$ (2, p_2+1), with $t_{1\_2}=h_1$, $t_{2\_p2+1}=p_2h_2=T_2$. After that, we integrate one time step h_1 in respect of the slow time t_1 –assigning to $\hat{\boldsymbol{x}}$ (2, 1) the value of $\hat{\boldsymbol{x}}$ (2, $p2$+1) – and then we start again the integration process on the row 3 (in respect of the fast time t_2) from the column 2 to the column p_2+1, and so on until we arrive in the point $\bar{t}(p_1+1,p_2+1)=(t_{1\_p_1+1},t_{2\_p_2+1})$, with $t_{1\_p1+1}=p_1h_1=T_1$ and $t_{2\_p2+1}=p_1h_2p_2=p_1T_2$.

Remark 1. Before passing to the integration for the next grid (each grid having the size (p_1+1)x(p_2+1)), starting from the point $\bar{t}$ (p_1+2,2)=(t_{1_p1+2},t_{2_2}), with t_{1_p1+2}=(p_1+1)h_1, t_{2_2}=p_1T_2+h_2, we must consider the following boundary conditions:
$\hat{\boldsymbol{x}}(p_1+2,1)=\hat{\boldsymbol{x}}(p_1+1,p_2+1)$; $\hat{\boldsymbol{x}}(p_1+i,1)=$
$=\hat{\boldsymbol{x}}(p_1+i\text{-}1,p_2+1)$, $i=\overline{3,p_1+1}$ on the column t_2 = 0, and $\hat{\boldsymbol{x}}$ (p_1+1,j), $j=\overline{2,p_2+1}$ on the row t_1 = T_1. We continue integrating with the step h_1 in respect of the slow time t_1 from the point $\bar{t}(p_1+1,p_2+1)$ to the point $\bar{t}(p_1+2,2)$ (Fig. 1).

Proceeding in this way for the other grids we shall integrate the MPDE until the point $\bar{t}(n_1+1,p_2+1)=(t_{1\_n_1+1},t_{1\_p_2+1})$, with $t_{1\_n_1+1}=m_1T_1$, and $t_{2\_p_2+1}=n_1T_2$. At each time $\bar{t}$ (i,j) we have to solve a nonlinear algebraic equation system. For this, we can use the Newton-Raphson algorithm or other efficient numerical iteration algorithms [1-7, 13].

The discrete resistive circuit equations, associated with the BDF of the first order ($a_0=1$ and $a_1=-1$) when the characteristics of the nonlinear elements are

approximated by piecewise-linear continuous curves, at time moment $\bar{t}\,(i,j)$ and at the (k+1)th iteration of the Newton-Raphson algorithm, corresponding to the modified nodal analysis method, have the following form:

$$\begin{bmatrix} \boldsymbol{G}_{dn-1,n-1}\left(s_{(i,j)}^{(k)}\right) & \boldsymbol{B}_{dn-1,m}\left(s_{(i,j)}^{(k)}\right) \\ \boldsymbol{A}_{dm,n-1}^{(k+1)}\left(s_{(i,j)}^{(k)}\right) & \boldsymbol{R}_{dm,m}\left(s_{(i,j)}^{(k)}\right) \end{bmatrix} \begin{bmatrix} \boldsymbol{v}_{n-1(i,j)}^{(k+1)} \\ \boldsymbol{i}_{m(i,j)}^{(k+1)} \end{bmatrix} = \begin{bmatrix} \boldsymbol{i}_{sc,(i,j)}^{(k)} \\ \boldsymbol{e}_{m,(i,j)}^{(k)} \end{bmatrix}. \quad (5)$$

where: $\boldsymbol{G}_{dn-1,n-1}\left(s_{(i,j)}^{(k)}\right)$ is the incremental node-conductance matrix corresponding to the n–1 independent nodes; $\boldsymbol{B}_{dn-1,m}\left(s_{(i,j)}^{(k)}\right)$ is an $(n-1)\times m$ matrix containing the elements –1, 0, +1 and the current gains of the CCCSs; $\boldsymbol{A}_{dm,n-1}\left(s_{(i,j)}^{(k)}\right)$ represents a mx(n-1) matrix containing the elements –1, 0, +1 and voltage gains of the VCVSs; $\boldsymbol{R}_{dm,m}\left(s_{(i,j)}^{(k)}\right)$ is a $m\times m$ matrix having the entries made up of: the transfer resistances of the CCVSs; the incremental resistances of the discrete models of the current-controlled dynamic circuit elements and the incremental resistances of the current-controlled nonlinear resistors; $\boldsymbol{v}_{n-1(i,j)}^{(k+1)}$ is node-voltage vector corresponding to the n–1 independent nodes (at the (k+1)th iteration and the time moment $\bar{t}\,(i,j)$; $i_{m(i,j)}^{(k+1)}$ represents the current vector corresponding to the non-NA-compatible circuit branches at the (k+1)$^{\text{th}}$ iteration and the time moment $\bar{t}(i,j)$. The vectors $i_{sc,n-1(i,j)}^{(k)}$ and $e_{m(i,j)}^{(k)}$ represent the contributions of the excitation sources (independent current and voltage sources), of the sources corresponding to the approximations of nonlinear resistors and the initial values of capacitor voltages and inductor currents which are determined from previous time steps $\bar{t}(i-1,j)$ of the slow time t_1 and $\bar{t}(i,j-1)$ of the fast time t_2.

For the case when the circuit contains flux-controlled nonlinear inductors and charge-controlled nonlinear capacitors, we must consider as independent variables also the flux vector $\boldsymbol{\varphi}_{L(i,j)}^{(k+1)}$ and the charge vector $\boldsymbol{q}_{C(i,j)}^{(k+1)}$, respectively [5, 9].

In the following we present the contributions of some dynamic circuit elements to the modified nodal equation (5).

The voltage-controlled nonlinear capacitor $\hat{q}_C(u_C)$

The nonlinear characteristic $\hat{q}_C(u_C)$ is approximated by piecewise linear continuous curve:

$$q_C = C_d(s)\cdot u_C + Q_C(s);\ u_C^-(s) \le u_C \le u_C^+(s), \quad (6)$$

$$\begin{aligned} i_{C(i,j)}^{(k+1)} &= \mathrm{d}\,q_C/\mathrm{d}\,t = \left(q_{C(i,j)}^{(k+1)} - q_{C(i-1,j)}^{(k+1)}\right)/h_1 + \\ &+ \left(q_{C(i,j)}^{(k+1)} - q_{C(i,j-1)}^{(k+1)}\right)/h_2 = \\ &= \frac{h_1+h_2}{h_1h_2}\left[C_d\left(s_{(i,j)}^{(k)}\right)\cdot u_{C(i,j)}^{(k+1)} + Q_C\left(s_{(i,j)}^{(k)}\right)\right] - \\ &- \left[C_d\left(s_{(i-1,j)}^{(k)}\right)\cdot u_{C(i-1,j)}^{(k+1)} - Q_C\left(s_{(i-1,j)}^{(k)}\right)\right]/h_1 - \\ &- \left[C_d\left(s_{(i,j-1)}^{(k)}\right)\cdot u_{C(i,j-1)}^{(k+1)} - Q_C\left(s_{(i,j-1)}^{(k)}\right)\right]/h_2. \end{aligned} \quad (7)$$

It results that the contribution of the v.c. nonlinear capacitor to MNE (5) is:

	$v_{C(i,j)}^{+(k+1)}$	$v_{C(i,j)}^{-(k+1)}$
$v_{C(i,j)}^{+(k+1)}$	$\frac{h_1+h_2}{h_1h_2}C_d\left(s_{(i,j)}^{(k)}\right)$	$-\frac{h_1+h_2}{h_1h_2}C_d\left(s_{(i,j)}^{(k)}\right)$
$v_{C(i,j)}^{-(k+1)}$	$-\frac{h_1+h_2}{h_1h_2}C_d\left(s_{(i,j)}^{(k)}\right)$	$\frac{h_1+h_2}{h_1h_2}C_d\left(s_{(i,j)}^{(k)}\right)$

RHS

$-\frac{h_1+h_2}{h_1h_2}Q_C\left(s_{(i,j)}^{(k)}\right) + \left[C_d\left(s_{(i-1,j)}^{(k)}\right)\cdot u_{C(i-1,j)}^{(k+1)} - Q_C\left(s_{(i-1,j)}^{(k)}\right)\right]/h_1 + \left[C_d\left(s_{(i,j-1)}^{(k)}\right)\cdot u_{C(i,j-1)}^{(k+1)} - Q_C\left(s_{(i,j-1)}^{(k)}\right)\right]/h_2$
$\frac{h_1+h_2}{h_1h_2}Q_C\left(s_{(i,j)}^{(k)}\right) - \left[C_d\left(s_{(i-1,j)}^{(k)}\right)\cdot u_{C(i-1,j)}^{(k+1)} - Q_C\left(s_{(i-1,j)}^{(k)}\right)\right]/h_1 - \left[C_d\left(s_{(i,j-1)}^{(k)}\right)\cdot u_{C(i,j-1)}^{(k+1)} - Q_C\left(s_{(i,j-1)}^{(k)}\right)\right]/h_2$

The current-controlled nonlinear inductor $\hat{\varphi}_L(i_L)$

The nonlinear characteristic $\hat{\varphi}_L(i_L)$ is approximated by piecewise linear continuous curve:

$$\varphi_L = L_d(s)\cdot i_L + \phi_L(s)\ \square\ i_L^-(s) \le i_L \le i_L^+(s), \quad (8)$$

$$\begin{aligned} u_{L(i,j)}^{(k+1)} &= \frac{h_1+h_2}{h_1h_2}\left[L_d\left(s_{(i,j)}^{(k)}\right)\cdot i_{L(i,j)}^{(k+1)} + \phi_L\left(s_{(i,j)}^{(k)}\right)\right] - \\ &- \left[L_d\left(s_{(i-1,j)}^{(k)}\right)\cdot i_{L(i-1,j)}^{(k+1)} + \phi_L\left(s_{(i-1,j)}^{(k)}\right)\right]/h_1 - \\ &- \left[L_d\left(s_{(i,j-1)}^{(k)}\right)\cdot i_{L(i,j-1)}^{(k+1)} + \phi_L\left(s_{(i,j-1)}^{(k)}\right)\right]/h_2, \end{aligned} \quad (9)$$

and the contribution of this element to MNE (5) is:

	$v_{L(i,j)}^{+(k+1)}$	$v_{L(i,j)}^{-(k+1)}$	$i_{L(i,j)}^{(k+1)}$
$v_{L(i,j)}^{+(k+1)}$			+1
$v_{L(i,j)}^{-(k+1)}$			–1
$i_{L(i,j)}^{(k+1)}$	+1	–1	$-\frac{h_1+h_2}{h_1h_2}L_d\left(s_{(i,j)}^{(k)}\right)$

RHS

$-\left[L_d\left(s_{(i-1,j)}^{(k)}\right)\cdot i_{L(i-1,j)}^{(k+1)} + \phi_L\left(s_{(i-1,j)}^{(k)}\right)\right]/h_1 - \left[L_d\left(s_{(i,j-1)}^{(k)}\right)\cdot i_{L(i,j-1)}^{(k+1)} + \phi_L\left(s_{(i,j-1)}^{(k)}\right)\right]/h_2.$

3. EXAMPLE

We consider the simple neural network in Fig. 2. The input signals have the following expressions:

$$v_1(t) = 4\sin\left(2\pi 9.9910^8 t + \pi/2\right) \text{ V},$$
$$v_{34}(t) = 4\sin\left(2\pi 1.00110^9 t\right) \text{ V}.$$

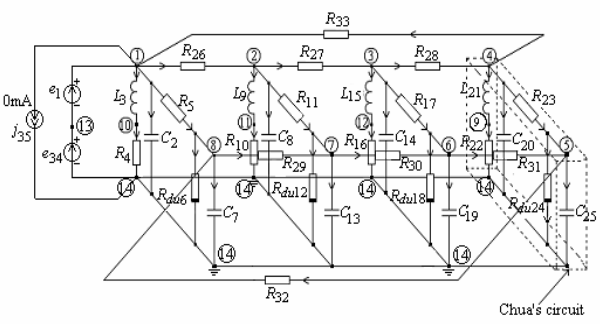

Fig. 2: Simple neural network.

The state vector for the circuit represented in Fig. 2 has the following structure:

State_vector:={UC11,IL16,IL9,IL23,IL2,UC6, UC13,UC18,UC20,UC25,UC27};

Eliminating the state variables **elm_stvar**: = {UC8_n, UC14_n, IL3_n, IL9_n, IL15_n, IL21_n}, and taking h_1=2us and h_2 = 0.05us, we obtain the reduced-order state equations:

Rem_st_eqs := {20.50*UC25_n-.5000*UC25_o1-20.00*UC25_o2 = .2000e-1*UC19_n-.9682e-1*UC25_n+.5682e-1*UC20_n-.1000***Gdu24(s)***UC25_n-.1000***ju24(s)**+.2000e-1*UC7_n,

20.50*UC7_n-.5000*UC7_o1-20.00*UC7_o2 = -.9682e-1*UC7_n+.2000e-1*UC13_n+.5682e-1*e1-.1000* **Gdu6(s)***UC7_n-.1000***ju6(s)**+.2000e-1*UC25_n,

20.50*UC20_n-.5000*UC20_o1-20.00*UC20_o2 = .4001*e1-.7982*UC20_n-.2439e-3*IL21_o1-.9756e-2* IL21_o2+.5682e-2*UC25_n+.1763e-3*UC8_o1+.7052e-2* UC8_o2+.9392e-2*UC14_o1+.3756*UC14_o2+.1067e-3* UC19_n-.1832e-3*IL15_o2-.8600e-7*IL9_o1-.3440e-5*IL9_o2-.4580e-5*IL15_o1+.2003e-5*UC13_n,

20.50*UC13_n-.5000*UC13_o1-20.00*UC13_o2 = -.9680e-1* UC13_n+.2000e-1*UC19_n+.2504e-4*UC14_o1+.1002e-2* UC14_o2+.2002e-4*UC20_n-.4886e-6*IL15_o2-.6506e-6*IL9_o1-.2603e-4*IL9_o2-.1222e-7*IL15_o1+.1067e-2*e1+.1334e-2* UC8_o1+.5335e-1*UC8_o2-.1000***Gdu12(s)***UC13_n-.1000* **ju12(s)**+.2000e-1*UC7_n,

20.50*UC19_n-.5000*UC19_o1-20.00*UC19_o2 = -.9680e-1* UC19_n+.2000e-1*UC25_n+.2504e-4*UC8_o1+.1002e-2* UC8_o2+.1334e-2*UC14_o1+.5335e-1*UC14_o2+.1067e-2* UC20_n-.2603e-4*IL15_o2-.1222e-7*IL9_o1-.4886e-6*IL9_o2-.6506e-6*IL15_o1+.2002e-4*e1+.2000e-1*UC13_n-.1000***Gdu18(s)***UC19_n-.1000***ju18(s)**}.

In these equations appear as the symbols and the parameters associated with the nonlinear circuit elements.

The slow component period is T_1=1000 ns, and the fast one is T_2= 1ns. To visualize the steady state by classical transient analysis, using a time step h=0.01 us, we need 10^6 samples to represent one period of the slow component. For a two-time representation of the signals a uniform grid of size 20×500 = 10^4 is enough. The variations of the output voltages v_6, v_{12}, v_{18}, and v_{24}, are shown in Fig. 3 in one-time variable representation when we use our computing program [2] and in Fig. 4 are represented the same variations when we use the Spice program.

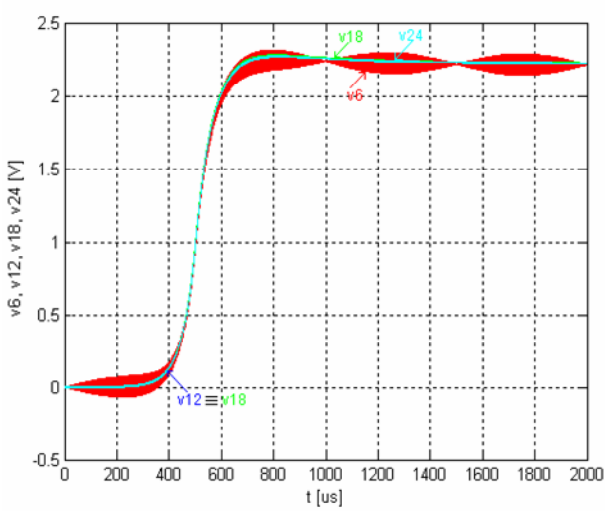

Fig. 3: One-time variation of the output voltage v_6 using our program.

For a bi-variate input signal $v_i(t)$ with the expression:

$$v_i(t_1, t_2) = 8\sin(2\pi 10^3 t_1)\sin(2\pi 10^6 t_2) \text{ V},$$

the output voltage v_6 is represented in two-time variable in Fig. 5, and in one-time variable in Fig. 6.

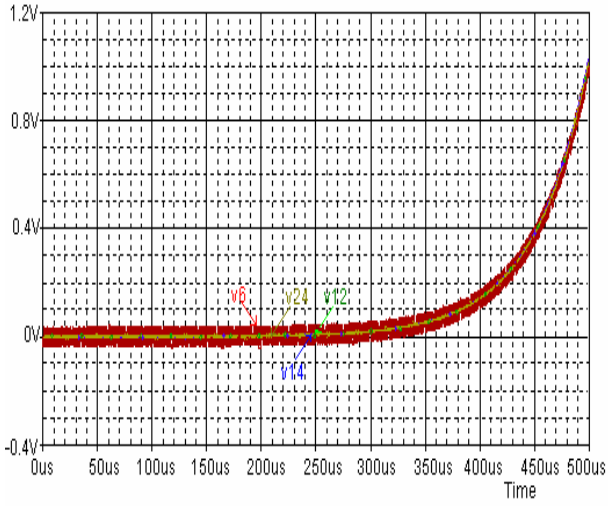

Fig. 4: One-time variation of the output voltage v_6 using Spice program.

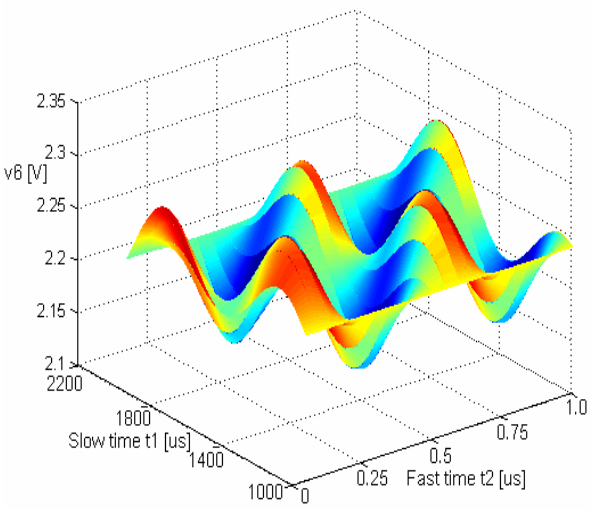

Fig. 5: Two-time variation of capacitor voltage $v_{C7}=v_{Rdu6}$.

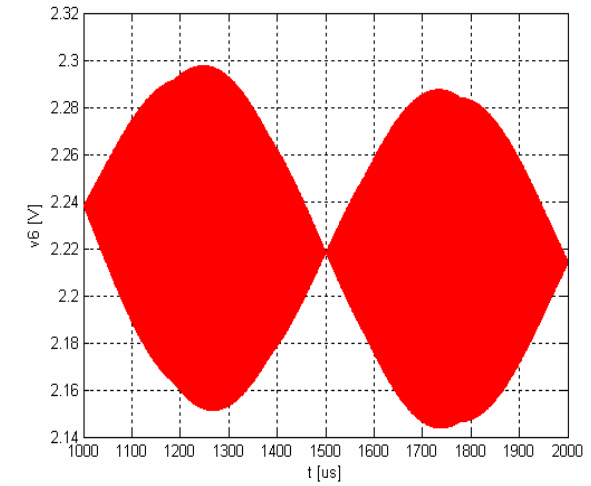

Fig. 6: One-time variation of capacitor voltage $v_{C7}=v_{Rdu6}$.

Representing the simulation results in two-time form is useful for visualizing the waveforms with widely separated time scales.

4. CONCLUSIONS

An efficient numerical approach for analyzing strongly nonlinear multirate circuits has been presented. The procedure uses multiple time variables to describe multirate behavior, leading to multi-time partial differential equations. The state equation formulation in a partially symbolic reduced form is used in order to obtain a MPDE form with a minimum number of independent variables. A new way to compute the appropriate BCs of the MPDE in order to accelerate the reaching of the periodic steady state is proposed. Combining this procedure with the state variable approach, in which only the symbols of the parameters corresponding to the nonlinear circuit elements are considered, a significant efficiency in circuit design and an improvement of the accuracy in the numerical calculations are obtained.

Acknowledgments

The research is financed from CNCSIS grants: C292 and C38.

References

[1] J. Roychowdhury, "Analyzing Circuits with Widely Separated Time Scales Using Numerical PDE Methods", IEEE Trans. on CAS – I, Vol. 48, N0. 5, May 2001, pp. 578-594.

[2] Fl. Constantinescu, Miruna Nitescu, "A new multi-rate method for analysis of RF-IC circuits", Proc. of the International Symposium on Signals, Circuits and Systems, SCS'03, Iasi, Romania, July, 10-11, 2001, pp. 91-94.

[3] H. G. Brachtendorf, G. Welsch, R. L. Laur, "A novel time-frequency method for the simulation of the steady state of circuits driven by multi-tone signals", Proc. on ISCAS, June 9-12, 19977, Hong Kong, pp.1508-1511.

[4] C.W. Ho, A. E. Ruehli, P. A. Brennan, "The modified nodal approach to network analysis", IEEE, Trans., CAS, 22, *5*, 1975, pp. 504-509.

[5] A. E. Schwarz, *Computer-aided design of microelectronic circuits and systems*, Academic Press, London, 1987.

[6] L. O. Chua, and P. M. Lin, *Computer-Aided Analysis of Electronic Circuits: Algorithms and Computational Techniques*, Englewood Cliffs, NJ:Prentice-Hall, 1975.

[7] A. Ushida, L. O. Chua, "Frequency-domain analysis of nonlinear circuits driven by multi-tone signals", IEEE Trans. on Circuits and Systems , Vol. CAS-31, No. 9, Sept. 1984, pp. 766-779.

[8] M. Iordache, M. Perpelea, "Modified nodal analysis for large-scale piecewise-linear nonlinear electric circuits", Rev., Roum., Sci., Techn., Électrotechn. et Énerg., 37, No. 4, Bucarest, 1992, pp. 487-496.

[9] M. Iordache, Lucia Dumitriu, L. Mandache, "Time-Domain Modified Nodal Analysis for Large-Scale Analog Circuits", Revue Roum. Sci. Techn.- Électrotechn. et Énerg., Bucarest , Tome 48, No. 2-3 , Bucarest , 2003, pp. 257-268, RM-ISSN 0035-4066.

[10] M. Iordache**,** Lucia Dumitriu**, "**Efficient Decomposition Techniques for Symbolic Analysis of Large – Scale Analog Circuits by State Variable Method", Analog Circuits and Signal Processing, Kluwer**,** Vol. 40, No. 3, September 2004, Kluwer Academic Publishers, pp.235-253, ISSN:0925-1030.

[11] Angela M. Hodge, R. W. Newcomb, "Semistate Theory and Analog VLSI Design", IEEE Circuit and Systems Magazine, Vol. 2, No. 2, Second Quarter 2002, pp.30-49.

[12] L. Mandache, M. Iordache, Lucia Dumitriu, "Time-Domain Modified Nodal Analysis for Analog Circuits", Proceeding of 7th International Workshop on Symbolic Methods and Applications in Circuit Design, SMACD 2002, October 10-11, 2002, Sinaia, Romania.

[13] R. Achar, M.S. Nakhla, "Simulation of High-Speed Interconnects", Proceeding of the IEEE, Vol. 89, No. 5, May 2000, pp. 693-728.